Friction

Review Article

Enhancing friction in rubber treads under lubrication: A review

Arata Ishizako[1,✉], Toshiaki Nishi[1], Takeshi Yamaguchi[1,2]

Cite this article: Ishizako A, Nishi T, Yamaguchi T. *Friction* 2026, **14**(5): 9441202. https://doi.org/10.26599/FRICT.2025.9441202

ABSTRACT: Rubber products used in shoe soles and tires require high friction, especially under lubrication, to ensure safety in daily life. The frictional behavior of rubber under lubrication is influenced by various parameters, including the properties of the rubber tread, the lubricant, the mating surface, and the sliding conditions. The effects of these parameters on friction have been investigated, but the mechanisms for enhancing friction under lubrication have not been studied systematically. This review provides a summary of the methods used to enhance rubber friction under lubrication, including optimizing the tread groove geometry to improve drainage, increasing the contact area, preventing liquid from flowing into the contact interface, increasing hysteresis friction, and controlling the surface free energy of rubber to promote dewetting. Additionally, suction-based attachment is emphasized as an effective mechanism for liquid-covered surfaces. Integrating these approaches may significantly advance the design of high-friction rubber treads, enabling the development of materials that maintain high friction regardless of lubrication conditions.

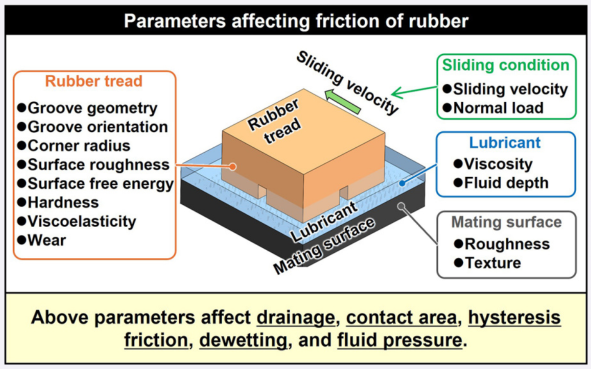

KEYWORDS: rubber; lubrication; friction; tread groove; texture; dewetting

1 Introduction

Soft materials, such as polymers, gels, foams, and biomaterials [1], have characteristically low elasticity and deform easily under the influence of external forces, even at room temperature [2, 3]. Rubber is a polymer with unique friction and sealing properties, and it has a wide range of industrial applications, including tires [4], shoes [5], robotic fingers [6], wiper blades [7], and mechanical seals [8].

Rubber materials have greater friction than other materials under dry conditions because of their high adhesion friction [9, 10] and hysteresis friction [10, 11]. Adhesion friction, which is the product of the real contact area and interfacial shear strength, is necessary to shear the bonds formed at a contact interface [9]. Hysteresis friction is caused by energy loss associated with the internal damping effects within a viscoelastic body. When a viscoelastic elastomer slides against a rough surface, hysteresis friction is dominant. In contrast, when the mating surface is smooth, adhesion friction is the main source of friction [12]. However, the friction coefficient of rubber decreases under liquid lubrication [12, 13]. Under such lubrication conditions, a liquid film forms at the contact interface because of the fluid pressure generated by the wedge and squeeze action [14]. The boundary, mixed, and hydrodynamic lubrication regimes are influenced by the lubricant viscosity, sliding velocity, and contact pressure, respectively [15]. The contact pressure between hard materials, such as metals, is typically approximately 3–4 GPa, whereas that between soft materials, such as rubber, is as low as 1 MPa [16], facilitating the formation of liquid films at the contact interface [17]. Consequently, adhesion friction significantly decreases, leading to low friction under liquid lubrication [12].

Enhancing the friction of soft materials under lubrication is crucial for real-world applications. For example, the frictional properties of tires directly affect automobile safety. The risk of traffic accidents increases on road surfaces with low skid resistance [18–20]. On wet roads, the skid resistance decreases by approximately 20%, resulting in lower friction and thus a greater risk of traffic accidents [21, 22]. Accordingly, many studies have been conducted on the prevention of hydroplaning, where the surfaces of a tire and the road are separated by a high-pressure water film [23–28]. Similarly, the friction properties of shoe soles help determine the risk of slip-and-fall accidents. Falls are a leading cause of occupational injuries worldwide [29–32], with slip-induced falls accounting for approximately 40% of total fall-related accidents in 2011 [32]. Slip-induced falls are more likely to occur on wet surfaces because of the reduced friction between shoe soles and the ground under wet conditions [32–37]. Furthermore, grippers are often required in robotics to handle objects covered in water, soap, oil, or biofilms [38]. Objects are difficult to grasp with sufficient strength and reliability under

[1] Graduate School of Engineering, Tohoku University, Sendai 980-8579, Japan. [2] Graduate School of Biomedical Engineering, Tohoku University, Sendai 980-8579, Japan.

✉ Corresponding author. E-mail: arata.ishizako.a1@tohoku.ac.jp

Received: July 17, 2025; Revised: October 23, 2025; Accepted: December 3, 2025

slippery contact conditions. Increasing the normal force to ensure that the grip is not always viable, especially when handling fragile objects. Therefore, maintaining a high friction coefficient under lubrication is essential across various fields.

In summary, the friction of rubber treads under liquid lubrication should be enhanced to improve safety in daily life. Rubber friction under lubrication is influenced by various parameters, such as the properties of the rubber tread, the lubricant, the mating surface, and the sliding conditions (Fig. 1). Although these factors have been investigated, the mechanisms by which friction can be enhanced under liquid lubrication have not been systematically clarified. Therefore, the strategies for increasing the friction of rubber materials under lubrication should be comprehensively understood.

In this review, we summarize methods for enhancing the friction of rubber used in shoe soles, tires, and robotic hands under lubrication. Furthermore, on the basis of this review, we identify current challenges and propose future research directions for enhancing rubber friction in wet environments.

2 Parameters affecting friction enhancement

2.1 Tread geometry

Tread geometry influences friction under lubrication; different tread designs exhibit varying frictional properties, primarily due to their drainage capabilities. Hemler et al. [39] conducted friction tests on shoe soles that were worn with an abrasive belt under glycerol solution lubrication. They reported that the friction coefficient decreased and the fluid force at the interface increased as the shoes became more worn. This was attributed to the disappearance of tread grooves with wear, which inhibited drainage at the contact interface. Consequently, liquid remained at the interface, increasing fluid pressure and reducing friction. Other studies have shown that the disappearance of grooves increases fluid pressure [40–42] and decreases friction [39, 43–50]. Therefore, efficient drainage through tread grooves is crucial for maintaining or enhancing friction under lubrication. Several parameters influence drainage performance, including the tread groove width [51–53], the tread groove depth [54, 55], the tread groove orientation [24, 25, 55–57], the edge shape of the tread block [58–60], and the roughness of the tread block's bottom surface [61, 62].

The width and depth of tread grooves affect the volume of drainable liquid, with larger groove dimensions being associated with higher friction coefficients [51–54]. Gupta et al. [52, 53] reported that the friction coefficient of shoes under water lubrication increased with the tread groove width (Fig. 2). Additionally, Li et al. [54] conducted friction tests on rubber treads with varying groove depths on different floors under water, detergent, and oil lubrication. They reported that deeper grooves promoted drainage and increased friction, particularly under water and detergent lubrication. Thus, increasing the width and depth of tread grooves enhances drainage and reduces the positive fluid pressure at the contact interface, thereby enhancing friction (Fig. 3). Notably, these experiments were conducted under high normal load conditions to simulate shoe-wear environments, as drainage contributes to friction under such high-load conditions.

The orientation of tread grooves influences the flowability of liquid at the contact interface, and friction tends to increase under water lubrication when the longitudinal direction of the tread groove is perpendicular to the sliding direction [24–56]. Li and Chen [56] conducted friction tests on rubber treads with different tread groove orientations under water, detergent, and oil lubrication. Here, rubber treads with grooves oriented perpendicular or at a 45-degree angle to the sliding direction (Fig. 4) exhibited better drainage and greater friction coefficients than rubber treads with grooves aligned parallel to the sliding direction, particularly under water and detergent lubrication. Blanchette and Powers [57] also investigated the effect of groove orientation on

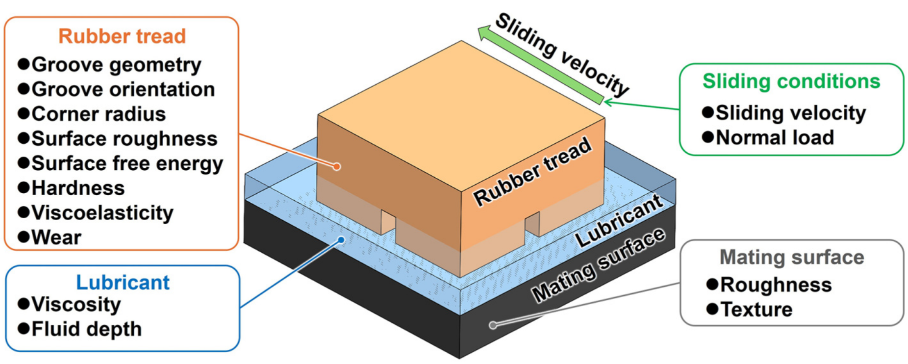

Fig. 1 Parameters affecting friction of rubber.

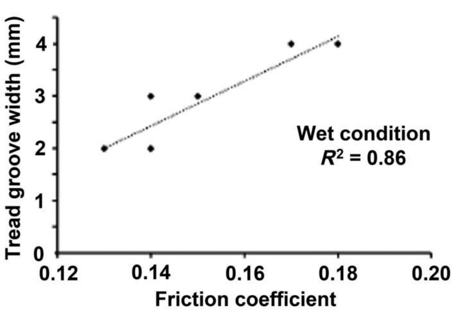

Fig. 2 Effect of tread groove width on friction coefficient under wet conditions. Reproduced with permission from Ref. [53], © The authors 2023.

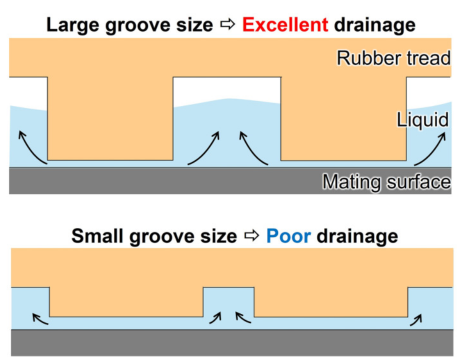

Fig. 3 Schematic diagram of effect of groove size on drainage performance.

the friction of shoe soles under water lubrication. Compared with grooves oriented perpendicular to the sliding direction, those inclined at 45 degrees in the sliding direction resulted in greater friction. Furthermore, researchers have used computational fluid dynamics (CFD) to investigate the relationship between tire grooves and hydroplaning risk [24–26] and reported that perpendicular grooves were less prone to hydroplaning than parallel grooves because they provided more efficient drainage. Specifically, vertically intersecting groove patterns reduce hydroplaning risk by increasing the effective groove volume. These simulation results indicate that improved drainage effectively maintains friction and reduces hydroplaning under high-speed sliding conditions.

The edge shape and surface roughness of the rubber tread affect liquid accessibility from the leading edge of the tread block. Through friction tests and contact surface observations of rubber treads with different end-face corner radii under glycerol lubrication, Ishizako et al. [58–60] reported that the friction coefficient increased as the end-face corner radius decreased. As shown in Fig. 5, under glycerol lubrication, samples with smaller corner radii exhibited greater friction than those with larger corner radii. Moreover, the difference in the friction between the two increased significantly with increasing sliding velocity [60]. Thus, a smaller end-face corner radius reduced fluid flow into the contact interface, resulting in a thinner film and/or larger contact area, thereby enhancing friction. Yamaguchi et al. [61] investigated the effect of the surface roughness of rubber treads under 90 wt% glycerol solution lubrication on a smooth stainless-steel plate. They reported that a smooth rubber tread (R_a = 0.98 μm) exhibited a low static friction coefficient and a high kinetic friction coefficient, whereas a rough rubber tread (R_a = 30.4 μm) showed high static and low kinetic friction coefficients. Furthermore, combining smooth and rough tread surfaces increased both friction coefficients. Using the total reflection method, the authors reported that rough-surface rubber had a larger contact area at the initiation of slip than smooth-surface rubber, but the opposite result was observed during steady-state sliding. They explained that the high static friction in the rough-surface sample was due to the breakdown of the lubricant film at the asperity tips caused by the high local contact pressure. In contrast, the high kinetic friction in the smooth-surface sample was attributed to its leading edge, which inhibited the infiltration of the glycerol solution into the contact interface during sliding. This effect was also confirmed in a study involving actual shoes [62].

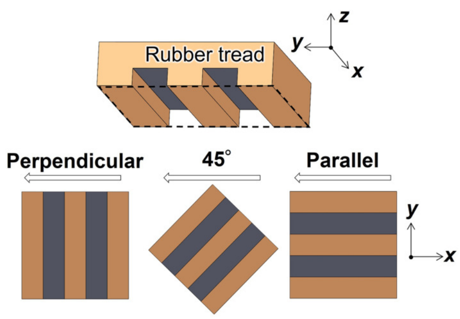

Fig. 4 Schematic diagram of tread groove orientation.

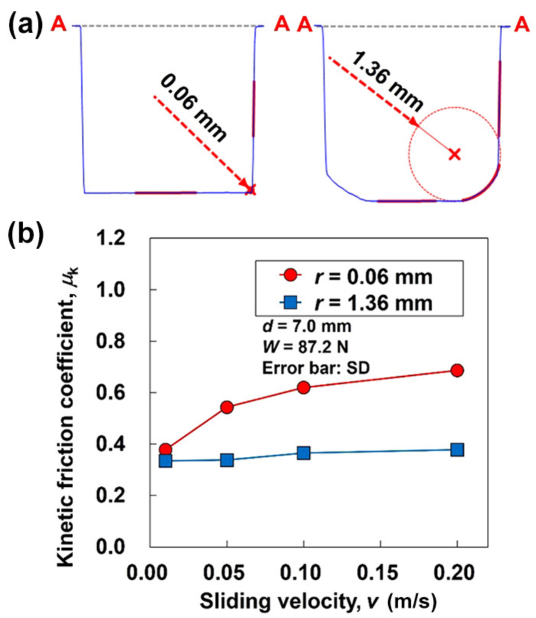

Fig. 5 Effect of end-face corner radius on friction coefficient under glycerol lubrication. (a) Cross-sectional profiles of tread blocks with different end-face corner radii *r*. (b) Effect of sliding velocity on kinetic friction coefficient. Reproduced with permission from Ref. [59], © Elsevier Ltd. 2023.

These findings indicate the importance of designing rubber treads that enhance drainage for high friction under lubrication. However, enlarging tread grooves reduces the stiffness of the rubber tread, thereby decreasing the contact area. Therefore, simply designing large grooves is insufficient. Maegawa et al. [63] conducted friction tests on rubber treads with varying numbers of grooves and surface roughness levels under mineral oil lubrication. The kinetic friction coefficient increased with the number of grooves in the samples with rough surfaces (R_a = 12.0 μm), whereas the kinetic friction coefficient of the samples with smooth surfaces (R_a = 0.15 μm) decreased with increasing groove number. For a rough mating surface, the localized contact pressure at the leading edge of the contact interface increased with the number of grooves, thus enhancing drainage; for a smooth mating surface, the real contact area of each tread block decreased as the number of grooves increased. Through friction tests on rubber treads with different groove heights and orientations on glass surfaces under glycerol solution lubrication, Yamaguchi et al. [55] reported that a thin tread block (height: 2 mm) with grooves parallel to the sliding direction yielded the highest friction coefficient. This result contradicts the friction test results obtained by Li et al. [54] and Li and Chen [56] under water and detergent lubrication. Yamaguchi et al. [55] reported that as the stiffness of a rubber tread decreased, the blocks became more easily deformed by frictional torque [64–66], thus reducing the contact area and friction. These findings suggest the presence of a trade-off between drainage and the real contact area of a rubber tread. Therefore, the optimal tread groove geometry for achieving high friction likely depends on the specific lubrication conditions.

The influence of the tread geometry of the rubber block on friction under lubrication is summarized in Table 1.

2.2 Material properties

Various fillers, such as carbon black, silica, and calcium carbonate, are often added to rubber to improve its mechanical and viscoelastic properties [67, 68]. Mechanical properties, such as hardness, influence the contact area between the rubber and the mating surface, whereas viscoelastic properties influence hysteresis friction. In addition, the surface free energy of rubber varies depending on the rubber type [69] and the filler type [70, 71]. The surface free energy influences the drainage of the thin liquid film at the contact interface by dewetting. Therefore, the effects of rubber material properties on friction enhancement should be clarified.

Table 1 Summary of studies on influence of tread geometry on friction under lubrication

Study (year)	Variable	Lubricant	Normal load/ contact pressure	Sliding velocity	Major result
Li and Chen (2004) [51]	Tread groove width	Water, detergent, and vegetable oil	—/—	—	Tread grooves should be sufficiently wide to ensure better drainage.
Gupta et al. (2023) [52]	Tread width and gap	Water	250 N/—	0.50 m/s	Large tread gaps enhance traction performance.
Gupta et al. (2023) [53]	Tread width and gap	Water	250 N/—	0.50 m/s	Large tread gaps improve traction performance.
Li et al. (2006) [54]	Tread groove depth	Water, detergent, and vegetable oil	44.5 N/—	—	Deep tread grooves provide high friction.
Yamaguchi et al. (2017) [55]	Tread block orientation and groove depth	Glycerol solution	66 N/264 kPa	0.20 m/s	Parallel and thin tread grooves exhibit high friction.
Li and Chen (2005) [56]	Tread groove orientation and width	Water, detergent, and vegetable oil	—/—	—	Perpendicular and oblique grooves exhibit high friction.
Blanchette and Powers (2015) [57]	Tread groove orientation, width, and depth	Water	400 N/—	0.50 m/s	Oblique grooves exhibit high friction.
Ong and Fwa (2007) [24]	Tread groove width, height, and orientation	Water	—/—	> 80 km/h	Simulations showed that perpendicular grooves have higher skid resistance than parallel grooves.
Fwa et al. (2009) [25]	Tread groove pattern	Water	2.41 kN/—	> 80 km/h	Simulations showed that perpendicular grooves have higher skid resistance than parallel grooves.
Kumar et al. (2009) [26]	Tread groove pattern	Water	2.41 kN/—	> 80 km/h	Simulations showed that a combination of perpendicular and parallel grooves improves skid resistance.
Ishizako et al. (2022) [58]	Lubricant viscosity and end-face corner radius	Glycerol solution	38.2 N/—	0.01–0.20 m/s	Small end-face corner radii result in high friction.
Ishizako et al. (2023) [59]	End-face corner radius	Glycerol	38.2 N/—	0.01–0.20 m/s	Friction increases as the corner radius decreases.
Ishizako et al. (2024) [60]	End-face corner radius	Glycerol	87.2 N/70 kPa	0.01–0.20 m/s	Small end-face corner radii result in high friction.
Yamaguchi et al. (2012) [61]	Surface roughness of rubber tread	Glycerol solution	56.6 N/90.5 kPa	0.20 m/s	Rubber blocks with rough and smooth surfaces exhibit high static and kinetic friction.
Yamaguchi and Hokkirigawa (2014) [62]	Surface roughness of rubber tread	Glycerol solution	514.5 N/—	< 0.50 m/s	Shoe soles with rough and smooth surfaces exhibit high static and kinetic friction.
Maegawa et al. (2016) [63]	Number of tread grooves	Mineral oil	30 N/—	0.1–10.0 mm/s	The effect of grooves on kinetic friction depends on the surface roughness of the rubber slider.

Rubber hardness influences the contact area and contact pressure. In particular, a lower hardness results in a larger contact area and greater friction [72–74]. Gupta et al. [73] conducted friction tests on commercial shoe soles with different hardness levels under water and detergent lubrication. They reported that the friction coefficient increased as the Shore hardness of shoe soles decreased (Fig. 6). Thus, softer shoe soles deform more easily to conform to the mating surface, thereby increasing the contact area and friction, as shown in Fig. 7. In addition, friction tests conducted under high-normal-load conditions using commercially available shoes indicate that rubber hardness effectively enhances friction under such conditions. However, a decrease in rubber hardness does not necessarily increase the friction coefficient. For example, Walter et al. [48] conducted friction tests on shoe soles with identical designs but different hardness levels on a tiled floor under glycerol solution lubrication. They reported no significant effect of rubber hardness on friction. Hence, as in the experiments of Walter et al. [48], the friction coefficient remains unchanged under high-viscosity liquid lubrication because the liquid is less easily drained from the contact interface.

The viscoelastic properties of rubber are critical for achieving high friction through hysteresis friction when it contacts a rough mating surface under lubrication. The viscoelasticity of rubber is characterized by a complex elastic modulus, which includes the

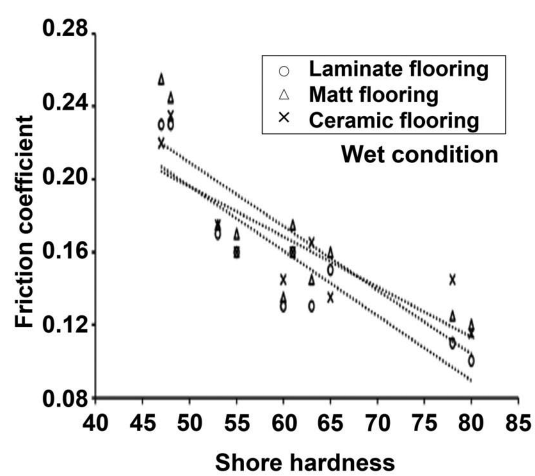

Fig. 6 Effect of Shore hardness on friction coefficient under wet conditions. Reproduced with permission from Ref. [73], © The authors 2022.

storage elastic modulus and loss elastic modulus. Persson [75] proposed a theory of rubber friction and contact mechanics on hard, rough surfaces, demonstrating that the friction coefficient due to hysteresis friction could be calculated via the viscoelastic properties of the rubber and the power spectral density of the surface roughness. This theory has been validated by several studies. Conducting friction tests between rubber and asphalt blocks under water lubrication, Lorenz et al. [76] reported good agreement between the rubber friction calculated via Persson's contact mechanics theory and adhesion theory and the corresponding measurements at low sliding velocities (< 0.001 m/s). Liu et al. [77] estimated the friction coefficient between tires and asphalt under water lubrication using Persson's theory and reported good agreement between the calculated and measured values at sliding velocities of 5–20 m/s. He et al. [78] integrated Persson's theory with CFD simulations and identified a strong correlation between the calculated and experimental results. Similarly, Ing et al. [79] applied Persson's theory to estimate the friction coefficient between shoes and floors under oil lubrication and reported a good correlation between the calculated and measured values when the smallest-scale surface features were excluded from the roughness spectrum. On the basis of these theoretical and experimental findings, we consider approaches to enhancing rubber friction under liquid lubrication. According to Persson's theory, a higher loss elastic modulus and a lower complex elastic modulus lead to greater hysteresis friction. Therefore, a higher loss tangent (ratio of the loss elastic modulus to the storage elastic modulus) leads to greater hysteresis friction [80], as shown in Fig. 8. However, the loss tangent depends on the deformation frequency of rubber, which depends on the roughness and sliding velocity of the mating surface. Therefore, to achieve high friction, the rubber material should be designed to have a high loss tangent under the assumed road surface conditions and sliding velocity.

The surface free energies of rubber, lubricant, and mating surfaces affect wettability or microscopic drainage at the contact interface due to dewetting. Therefore, the surface free energy of rubber should be controlled to promote drainage from the contact interface and enhance friction. The stability of the liquid film depends on wettability, as quantified by the spreading coefficient S (Eq. (1)) [81, 82]:

$$S = \gamma_{SR} - (\gamma_{SL} + \gamma_{LR}) \tag{1}$$

where γ_{SR}, γ_{SL}, and γ_{LR} are the interfacial tensions between solid and rubber, solid and liquid, and liquid and rubber. If $S < 0$, then the liquid dewets. Figure 9 shows the relationship between S and

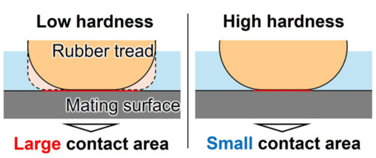

Fig. 7 Schematic diagram of relationship between rubber hardness and contact area.

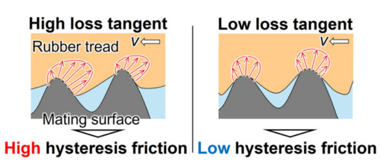

Fig. 8 Schematic diagram of relationship between loss tangent of rubber and hysteresis loss.

drainage by dewetting. Nishi et al. [83] conducted friction tests between isoprene rubber and a marble floor under water, ethanol, and glycerol lubrication using liquids with different surface free energies. They reported that a smaller S resulted in a higher dynamic friction coefficient (Fig. 10). Furthermore, maintaining nonuniform wettability across the rubber surface may enhance the dewetting effect. Nishi et al. [70] applied a hydrophilic hydrogel patch to hydrophobic silicone rubber and conducted friction tests on a silicone rubber hemisphere with nonuniform wettability under water lubrication. They reported that silicone rubber with a hydrogel patch size of 100 μm exhibited a higher friction coefficient than silicone rubber without the hydrogel patch under lubrication. In a subsequent study, Nishi et al. [71] confirmed that real contact formation in silicone rubber with a hydrogel patch was promoted by nonuniform wetting. Leveraging this mechanism for friction enhancement, they further developed rubber surfaces with nonuniform wettability by incorporating activated carbon and sodium chloride [84] and silicone rubber particles [85] to create microdimpled structures; these modifications enhanced friction. Therefore, maintaining nonuniform wettability on rubber surfaces promotes dewetting and enhances friction under lubrication. The influence of the material properties of the rubber block on friction under lubrication is summarized in Table 2.

2.3 Surface texture

As shown in Section 2.2, microscopic drainage influenced by surface free energy contributes to high friction, indicating the importance of real contact. To enhance real contact and achieve high friction under lubrication, researchers have explored

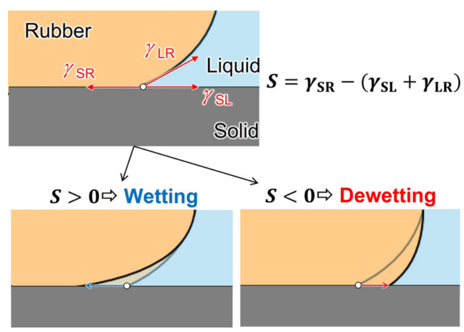

Fig. 9 Relationship between spreading coefficient and drainage by dewetting.

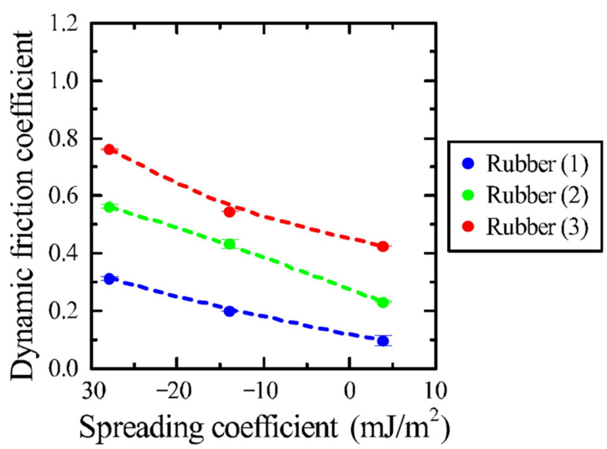

Fig. 10 Effect of spreading coefficient on dynamic friction coefficient. Reproduced with permission from Ref. [83], © Japanese Society of Tribologists 2016.

Table 2 Summary of studies on effects of material properties on friction under lubrication

Researcher (year)	Variable	Lubricant	Normal load/ contact pressure	Sliding velocity	Major result
Jones et al. (2018) [72]	Hardness and contact area of shoes	Water, detergent, and vegetable oil	250 N/—	0.5 m/s	Low-hardness shoe soles achieve high friction.
Gupta et al. (2022) [73]	Hardness and contact area of shoes	Water	270 N/—	0.5 m/s	Low-hardness shoe soles achieve high friction.
Walter et al. (2021) [48]	Hardness and worn region of shoes	Glycerol solution	250 N/—	0.5 m/s	No effects were observed due to shoe hardness.
Ido et al. (2019) [80]	Mating surface roughness and viscoelasticity	Water	—/1–3 MPa (pin on disk test)	1.0 m/s	High loss tangent and high surface roughness improve wet-grip performance.
Nishi et al. (2016) [83]	Spreading coefficient of lubricant	Water, ethanol, and glycerol	1.96 N/—	1.0–100.0 mm/s	Friction coefficients positively correlate with dewetting velocities.
Nishi et al. (2021) [70]	Hydrogel patch size	Water	0.098 N/138 kPa	0.10 mm/s	Silicone rubber with a 100-μm hydrogel patch achieves high friction.
Nishi et al. (2022) [84]	Content of rubber (carbon sodium)	Water	0.196 N/—	1.0 mm/s	Outsole materials filled with activated carbon or sodium chloride achieve high friction.
Nishi (2022) [85]	Content of rubber (silicone rubber particles)	Water	0.196 N/—	1.0 mm/s	Diene rubber containing silicone rubber particles exhibits high friction.

bioinspired textures, such as those of human fingerprints [86–89] and the legs of frogs and crickets [90–94].

Human fingerprints exhibit high friction coefficients under lubrication. Kim and Yun [86] demonstrated that the friction force of silicone rubber with rectangular fingerprint patterns under water lubrication was higher than that under dry conditions, suggesting that the presence of water in the fingerprint grooves generated additional adhesive force. Nishi et al. [87] conducted friction tests between a glass plate and an artificial skin block with a fingerprint pattern under water lubrication. They found reported higher friction under water lubrication than under dry conditions because real contact formation was promoted by negative pressure at the meniscus (Fig. 11). On the basis of these findings, fingerprint-inspired high-friction textures for robotic hands are being actively studied. Hao et al. [88] conducted object-grasping tests in water and oil using robotic hands with and without silicone rubber surfaces with fingerprint-like patterns (Fig. 12). They confirmed that the fingerprint-textured robot hand had a higher friction coefficient under lubrication.

Researchers are exploring the legs of species that live in wet environments. The toe pads of tree frogs are soft and have a regular hexagonal microstructure with a diameter of approximately 10 μm. The flattened surface of each cell has much finer microstructures (pegs with diameters of approximately 0.1–0.4 μm) originating from hemidesmosomes [95]. Persson [96]

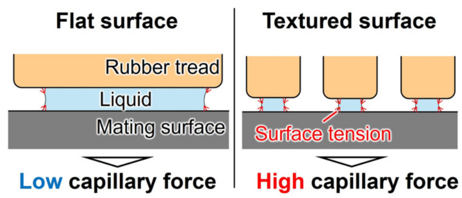

Fig. 11 Schematic diagram of difference in liquid film distribution depending on surface texture.

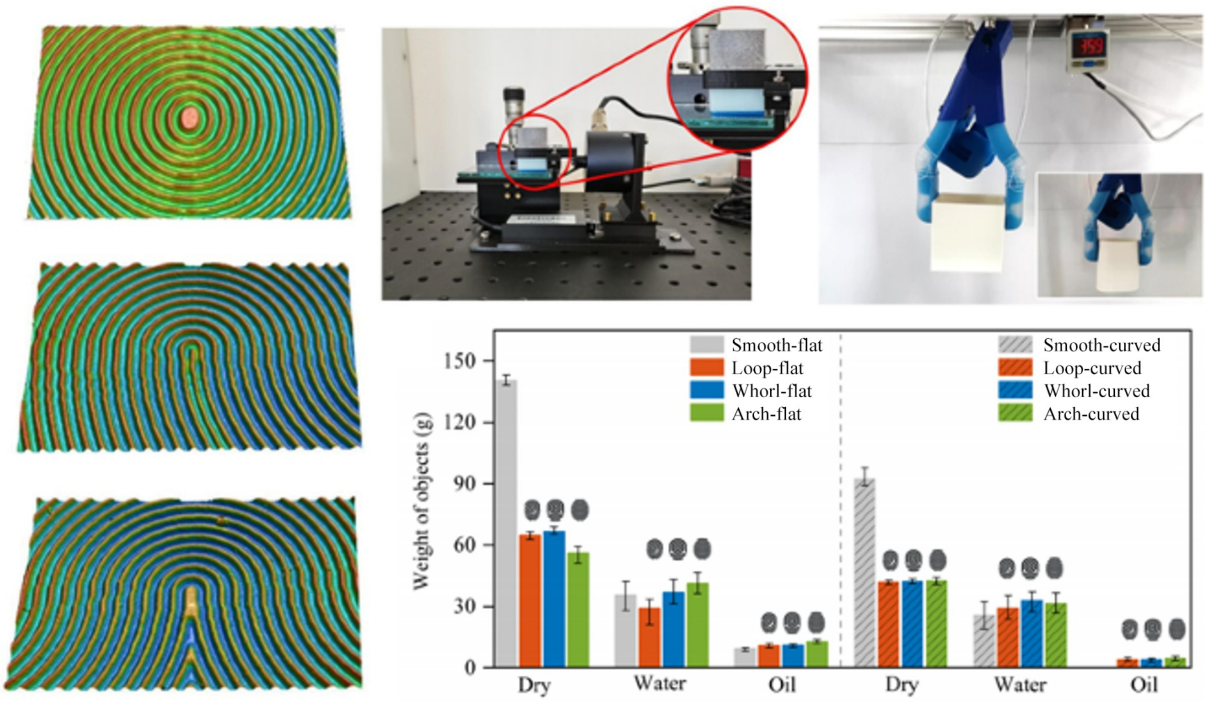

Fig. 12 Friction properties of fingerprint-inspired surface texture under water and oil lubrication. Reproduced with permission from Ref. [88], © The author(s) 2022.

developed a capillary bridge model and proposed a theory that frog-toe-pad channels serve three functions: reducing the bending elasticity of toe pads to increase the contact area; supplying liquid to the rough substrate surface for strong, fast adhesion; and facilitating drainage. On the basis of this theory, many studies have explored tread designs with hexagonal microgroove patterns inspired by frogs' toe pads [90–93, 97]. Zhang et al. [92] fabricated hexagonal textures with 10 μm diameters on a polydimethylsiloxane surface via ion etching, which was then rendered hydrophilic using oxygen plasma. The boundary friction in the textured sample was ~20 times higher than the dry or wet friction. Furthermore, Guo et al. [94] reported that the toe of a Chinese bush cricket features a unique hierarchical micro–nanostructure, where micropillars are embedded with long nanofibers and covered by smooth, thin films. Thus, they conducted friction tests using tread patterns simulating the cricket's toe and reported that the cricket-inspired pattern generated greater shear stress than the frog-inspired pattern under water lubrication (Fig. 13). The cricket-inspired pattern maintained a large liquid-film area because the rear side of the tread block did not peel off when the tread was deformed by friction forces. Bioinspired surface textures are expected to enhance friction, particularly in low-load applications such as medical devices and wearable electronics. However, under high-load conditions, this improvement may decrease because the effect of surface tension diminishes relative to the applied load.

A summary of studies on the effects of surface texture on friction under lubrication is presented in Table 3.

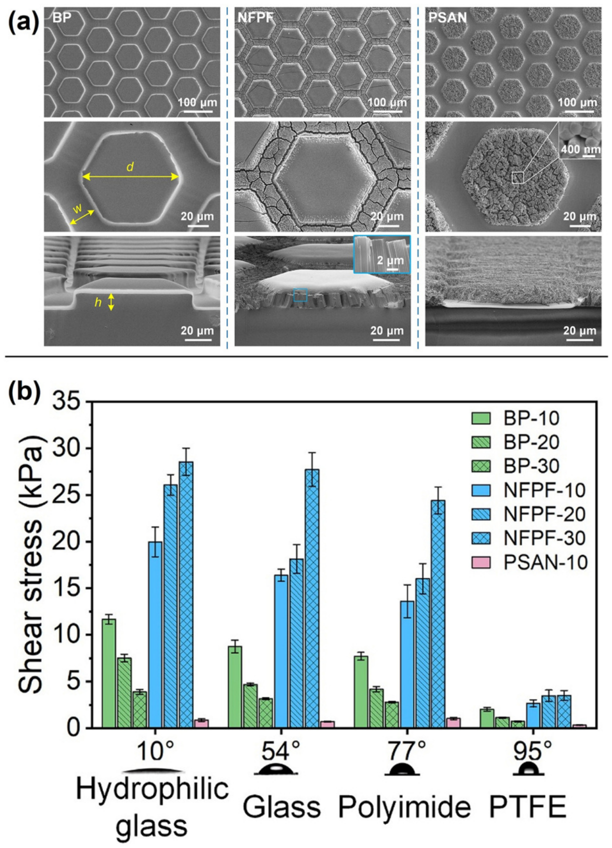

Fig. 13 Effects of bioinspired microtextures on friction coefficient under lubrication: (a) microscopy images of different types of pillars: a bulk pillar (BP) array, inspired by a tree-frog's toe; a nanofibrous pillar array covered with thin films (NFPF), inspired by a cricket's toe; and a hexagonal pillar array composed of self-assembled nanofibers (PSAN); (b) shear stress for different pillar surfaces. Reproduced with permission from Ref. [94], © The authors 2023.

3 Summary and research prospects

We summarize existing methods for enhancing rubber friction under lubrication, especially under wet conditions. The first step involves draining the liquid from the contact interface between the rubber and the mating surface. Effective drainage can be achieved by increasing the size of the tread grooves and orienting the tread longitudinally perpendicular to the sliding direction.

Moreover, liquid inflow from the front edge of the rubber block can be prevented by reducing the end-face corner radius while reducing the surface roughness of the rubber block. Additionally, micropatterns inspired by the body characteristics of species that inhabit wet environments can be designed to ensure efficient drainage and a large contact area. The material properties of rubber are also critical for increasing friction. Rubbers with a low hardness—i.e., a low storage elastic modulus—can easily deform to conform to the mating surface, thereby increasing the contact area and increasing adhesion and hysteresis friction. Rubbers with a high loss elastic modulus can exhibit high hysteresis friction due to increased energy dissipation. Furthermore, the contact area can be increased via the dewetting effect by controlling the surface free energy of the rubber. This effect can be induced by creating dimples or fingerprint-like patterns on the rubber surface, promoting bubble formation at the interface and establishing partial wetting conditions. Integrating these approaches can

Table 3 Summary of studies on effects of surface texture on friction under lubrication

Researcher (year)	Variable	Lubricant	Normal load/ contact pressure	Sliding velocity	Major result
Hao et al. (2023) [88]	Presence of fingerprint-like pattern	Water and oil	—/7.79 kPa	0.5 mm/s	Fingerprint-inspired surface textures achieve high friction under oil lubrication.
Hao et al. (2024) [89]	Presence of fingerprint-like pattern	Water, oil, and hyaluronic	—/2.39–11.79 kPa	—	Fingerprint-inspired surface textures achieve high friction under oil lubrication.
Drotlef et al. (2013) [90]	Micropillar geometry and wettability	Water	1 mN/—	5–200 μm/s	Tree-frog-like patterns lead to increased friction only when the liquid wets the surface.
Chen et al. (2015) [91]	Micropillar geometry	Water	3 mN/— 5000 mN/50 kPa	300 μm/s 500 μm/s	Hexagonal pillar patterns achieve improved wet friction performance.
Zhang et al. (2020) [92]	Bioinspired hierarchical pillar surface	Water	5 mN/—	200 μm/s	Boundary friction on bioinspired concave pillars can be 3.5 times higher than on a smooth surface.
Chen et al (2022) [93]	Frog-inspired tread pattern	Water	5–15 N/—	1.5–35 mm/s	Bionic hexagon tread pattern achieves high friction and directional stability.
Guo et al. (2023) [94]	Bioinspired hierarchical pillar surface	Water	Without applying additional force	200 μm/s	Unique hierarchical microfibrous–nanofibrous pillars, such as those inspired by bush cricket, achieve high friction.

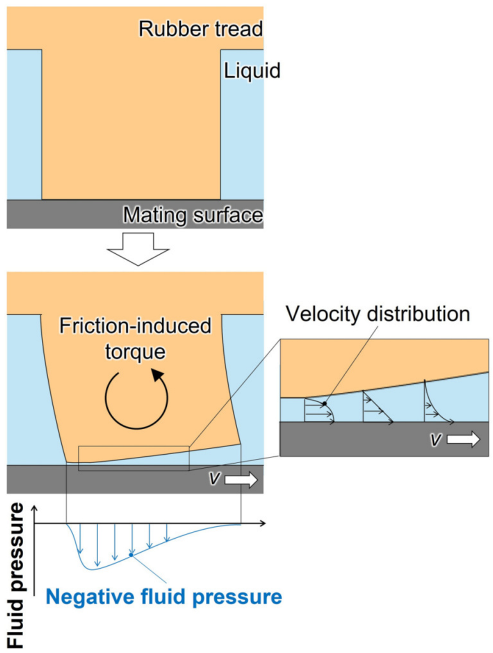

Fig. 14 Schematic of tread block deformation during sliding in liquid.

advance the design of high-friction rubber treads under wet conditions.

In recent years, alternative mechanisms for achieving high friction have been discovered or proposed under conditions involving highly viscous liquids, where the liquid is difficult to drain and van der Waals or capillary forces have limited effectiveness. Many aquatic species perform suction-based attachments, such as remora [98], octopus [99, 100], and gobies [101], in water. Given its effectiveness in water, this suction-based attachment mechanism has been used to develop transport devices. Wang et al. [98] reported that a remora-inspired adhesive disk generated high pull-off and friction forces in water. Baik et al. [99] measured the attachment force of silicone rubber whose texture resembled that of an octopus sucker under water and oil conditions and reported that it exhibited a greater attachment force than silicone rubber without such a texture. Furthermore, instead of relying on suction cups, researchers have reported that a negative dynamic pressure generated at the contact interface during sliding can increase friction [60, 102, 103]. Ishizako et al. [60, 102] conducted friction tests on rubber treads with varying end-face corner radii and different groove orientations under glycerol lubrication and measured the fluid pressure at the contact interfaces of the rubber treads. They reported that a negative fluid pressure was generated at the contact interface and that increasing

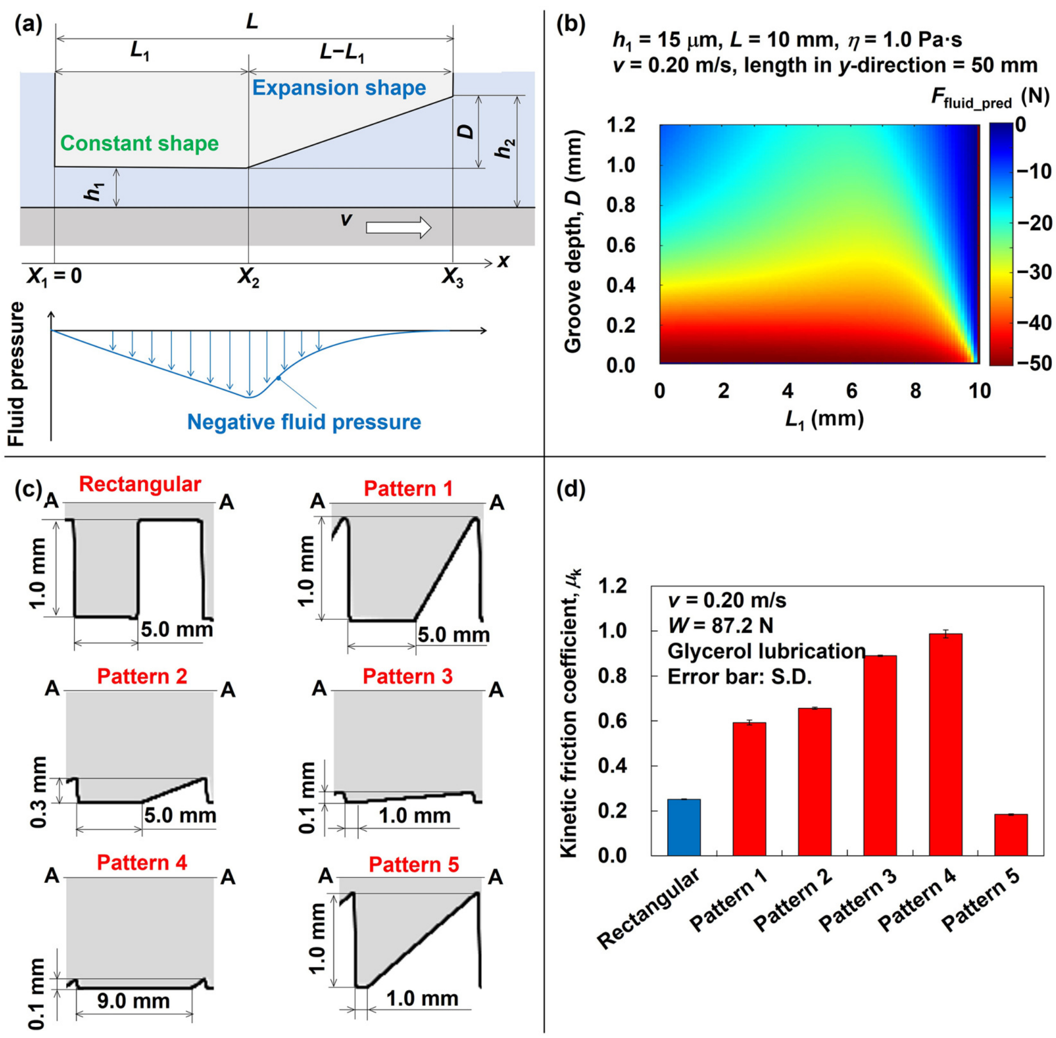

Fig. 15 Friction coefficient of inclined groove rubber tread: (a) schematic of flow channel model of tread block contact interface, (b) distribution of $F_{\text{fluid\_pred}}$ as a function of length of constant gap L_1 and groove depth D, (c) cross-sectional shape of each rubber tread sample, and (d) kinetic friction coefficient for each rubber tread sample. Reproduced with permission from Ref. [103], © The authors 2025.

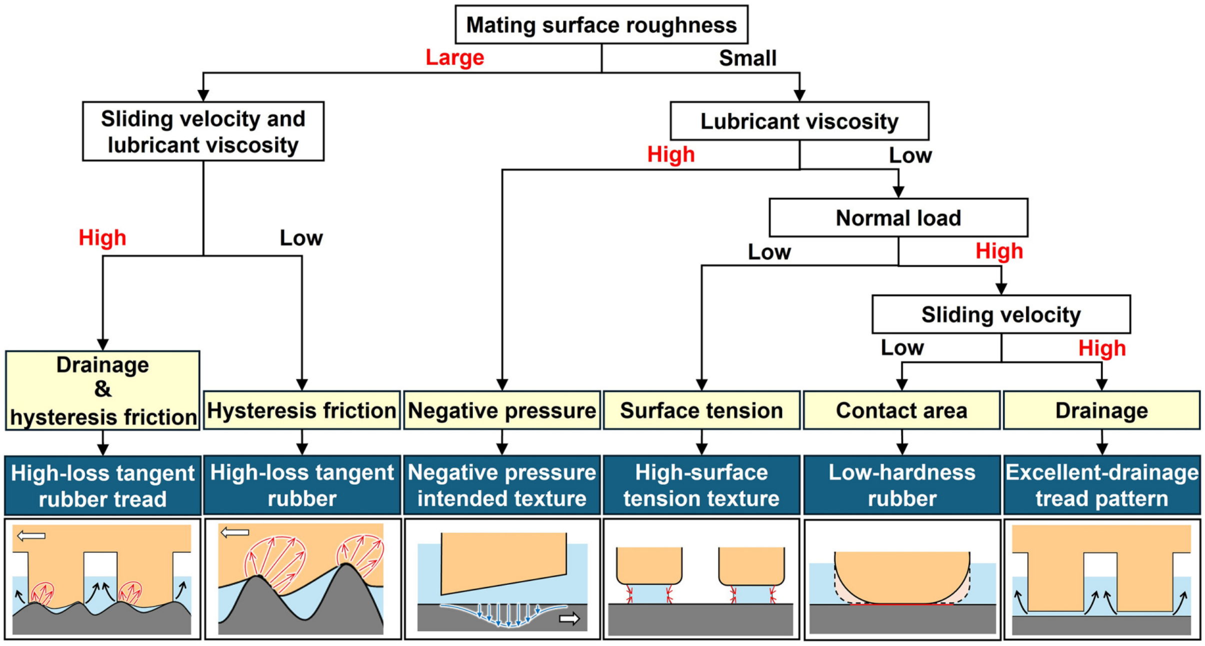

Fig. 16 Flowchart for enhancing friction approach.

the magnitude of this negative fluid pressure increased the friction coefficient. Figure 14 shows the deformation of a tread block during sliding in liquid. During sliding, the tread block deforms due to friction-induced torque [64–66]. Consequently, the rear side of the rubber tread peels off the mating surface, creating an expansion gap between the rubber tread and the mating surface. This gap promotes the generation of a negative fluid pressure through a mechanism opposite to wedge action [104, 105]. This negative fluid pressure reduces the liquid-film thickness during sliding, thereby increasing the real contact area, viscous resistance, and friction.

On the basis of these results, Ishizako et al. [103] proposed a tread design that intentionally generates negative fluid pressures via the abovementioned expansion gap mechanism. They conducted friction tests using a tread pattern with inclined tread grooves designed to generate a negative fluid pressure at the contact interface under glycerol lubrication. The friction coefficient of the inclined-groove rubber tread was up to four times greater than that of the rubber tread without inclined grooves (Fig. 15).

These approaches, which are based on adsorption forces, differ from conventional methods, which rely on drainage to increase friction. They are particularly effective in cases where the liquid is difficult to drain. Integrating these adsorption-based approaches into conventional friction-enhancing methods may lead to breakthroughs in the design of high-friction rubber treads, enabling the development of materials that maintain high friction regardless of lubrication conditions.

On the basis of the above literature review, we summarized previous efforts to improve friction in rubber treads in the flowchart shown in Fig. 16. When the mating surface is rough, the use of high-loss-tangent rubber increases hysteresis friction, thereby achieving high overall friction. However, under high-viscosity or high-sliding-velocity conditions, thick liquid films tend to form, reducing hysteresis friction; in such cases, promoting drainage is necessary to restore hysteresis friction. In contrast, when the mating surface is smooth, hysteresis friction does not occur, and a different approach is required to enhance adhesive friction. Specifically, high-viscosity lubricants have difficulty draining from the contact surface; in this situation, friction can be improved via fluid pressure control, i.e., generating negative fluid pressure. Conversely, with low-viscosity lubricants, drainage and surface-tension effects can be exploited. Under a low normal load, the influence of surface tension becomes more pronounced, making bioinspired high-tension surface textures—such as fingerprints and tree-frog's toe pads—effective in enhancing friction. Achieving optimal friction with these textures requires partial wetting conditions; when the liquid amount is excessive, fine menisci cannot form, reducing the friction enhancement. In addition, under high-load conditions, this improvement may decrease because the effect of surface tension diminishes relative to the applied load. Under a high normal load, maintaining a sufficient contact area becomes crucial; this can be achieved using low-hardness rubber or by improving drainage through tread pattern design. Improving drainage is particularly effective under high sliding-velocity conditions, where hydroplaning may occur.

Notably, the flowchart in Fig. 16 does not account for interactions among these factors. For example, improving drainage may increase hysteresis friction or surface-tension effects by reducing fluid film thickness, but introducing tread patterns for drainage may simultaneously reduce the contact area. Therefore, a tread pattern that provides high friction under certain conditions does not necessarily perform the same under different lubrication conditions. Future work should consider these complex interactions and evaluate friction from a multifaceted perspective to further enhance rubber performance.

Author contributions

Arata Ishizako: investigation, visualization, writing—original draft. Toshiaki Nishi: writing—review and editing. Takeshi Yamaguchi: supervision, writing—review and editing.

Availability of data and materials

Not applicable.

Declaration of competing interest

The authors have no competing interests to declare that are relevant to the content of this article.

References

[1] Bates F S, Fredrickson G H. Block copolymers: Designer soft materials. *Phys Today* **52**(2): 32–38 (1999)

[2] Li J, Wong W Y, Tao X M. Recent advances in soft functional materials: Preparation, functions and applications. *Nanoscale* **12**(3): 1281–1306 (2020)

[3] Calvert P. Hydrogels for soft machines. *Adv Mater* **21**(7): 743–756 (2009)

[4] Ramarad S, Khalid M, Ratnam C T, Chuah A L, Rashmi W. Waste tire rubber in polymer blends: A review on the evolution, properties and future. *Prog Mater Sci* **72**: 100–140 (2015)

[5] Rebenda D, Sáha T. Current state-of-the art review of footwear–ground friction. *Friction* **12**(10): 2188–2204 (2024)

[6] Shintake J, Cacucciolo V, Floreano D, Shea H. Soft robotic grippers. *Adv Mater* **30**(29): 1707035 (2018)

[7] Kaur H, Nirmal U. A review on the development of wiper system for automotive car windscreen cleaning application. *Curr J Appl Sci Technol* **41**(7): 1–27 (2022)

[8] Ke Y C, Yao X F, Yang H, Liu X Y. Kinetic friction characterizations of the tubular rubber seals. *Tribol Int* **72**: 35–41 (2014)

[9] Moore D F, Geyer W. A review of adhesion theories for elastomers. *Wear* **22**(2): 113–141 (1972)

[10] Persson B N J. On the theory of rubber friction. *Surf Sci* **401**(3): 445–454 (1998)

[11] Moore D F, Geyer W. A review of hysteresis theories for elastomers. *Wear* **30**(1): 1–34 (1974)

[12] Moore D F. A history of research on surface texture effects. *Wear* **13**(6): 381–412 (1969)

[13] Persson B N J, Tartaglino U, Albohr O, Tosatti E. Rubber friction on wet and dry road surfaces: The sealing effect. *Phys Rev B* **71**(3): 035428 (2005)

[14] Fernandez-Del-Rincon A, Diez-Ibarbia A, Theodossiades S. Gear transmission rattle: Assessment of meshing forces under hydrodynamic lubrication. *Appl Acoust* **144**: 85–95 (2019)

[15] Stribeck R. The essential properties of plain and roller bearings. *VDI Zeitschrift* **46**(37): 1341-1348 (1902) (in German)

[16] Höglund E. Influence of lubricant properties on elastohydrodynamic lubrication. *Wear* **232**(2): 176–184 (1999)

[17] Gaman I D C, Higginson G R, Norman R. Fluid entrapment by a soft surface layer. *Wear* **28**(3): 345–352 (1974)

[18] Asi I M. Evaluating skid resistance of different asphalt concrete mixes. *Build Environ* **42**(1): 325–329 (2007)

[19] Milton J C, Shankar V N, Mannering F L. Highway accident severities and the mixed logit model: An exploratory empirical analysis. *Accident Anal Prev* **40**(1): 260–266 (2008)

[20] Pardillo Mayora J M, Jurado Piña R. An assessment of the skid resistance effect on traffic safety under wet-pavement conditions. *Accident Anal Prev* **41**(4): 881–886 (2009)

[21] Adamu M, Mohammed B S, Shafiq N, Shahir Liew M. Skid Resistance of nano silica modified roller compacted rubbercrete for pavement applications: Experimental methods and response surface methodology. *Cogent Eng* **5**(1): 1452664 (2018)

[22] Stevens S E, Schreck C J, Saha S, Bell J E, Kunkel K E. Precipitation and fatal motor vehicle crashes: Continental analysis with high-resolution radar data. *B Am Meteorol Soc* **100**(8): 1453–1461 (2019)

[23] Cho J R, Lee H W, Sohn J S, Kim G J, Woo J S. Numerical investigation of hydroplaning characteristics of three-dimensional patterned tire. *Eur J Mech A—Solids* **25**(6): 914–926 (2006)

[24] Ong G P, Fwa T F. Effectiveness of transverse and longitudinal pavement grooving in wet-skidding control. *Transport Res Rec* **2005**(1): 172–182 (2007)

[25] Fwa T F, Kumar S S, Anupam K, Ong G P. Effectiveness of tire-tread patterns in reducing the risk of hydroplaning. *Transport Res Rec* **2094**(1): 91–102 (2009)

[26] Kumar S S, Kumar A, Fwa T F. Analyzing effect of tire groove patterns on hydroplaning speed. *J East Asia Soc Transp Stud* **8**: 2018–2031 (2009)

[27] Spitzhüttl F, Goizet F, Unger T, Biesse F. The real impact of full hydroplaning on driving safety. *Accident Anal Prev* **138**: 105458 (2020)

[28] Liu Y, Qian Z D, Liu C B, Huang Q B. Investigation on hydroplaning behaviors of a patterned tire on a steel bridge deck pavement. *Appl Sci* **11**(22): 10566 (2021)

[29] Strandberg L, Lanshammar H. The dynamics of slipping accidents. *Occup Accid* **3**(3): 153–162 (1981)

[30] Courtney T K, Sorock G S, Manning D P, Collins J W, Holbein-Jenny M A. Occupational slip, trip, and fall-related injuries can the contribution of slipperiness be isolated. *Ergonomics* **44**(13): 1118–1137 (2001)

[31] Kemmlert K, Lundholm L. Slips, trips and falls in different work groups—With reference to age and from a preventive perspective. *Appl Ergon* **32**(2): 149–153 (2001)

[32] Ohnishi A. Causes of occupational falls on the same level more than four days absence from work: Features based on monthly aggregation. *Jpn J Ergonom* **56**(3): 101–107 (2020)

[33] Bell J L, Collins J W, Wolf L, Grönqvist R, Chiou S, Chang W R, Sorock G S, Courtney T K, Lombardi D A, Evanoff B. Evaluation of a comprehensive slip, trip and fall prevention programme for hospital employees. *Ergonomics* **51**(12): 1906–1925 (2008)

[34] Drebit S, Shajari S, Alamgir H, Yu S C, Keen D. Occupational and environmental risk factors for falls among workers in the healthcare sector. *Ergonomics* **53**(4): 525–536 (2010)

[35] Verma S K, Chang W R, Courtney T K, Lombardi D A, Huang Y H, Brennan M J, Mittleman M A, Perry M J. Workers' experience of slipping in U. S. limited-service restaurants. *J Occup Environ Hyg* **7**(9): 491–500 (2010)

[36] World Health Organization. ISBN 978-92-4-002191-4. Step safely: Strategies for preventing and managing falls across the life-course, 2021.

[37] Shibata K, Ohnihsi A. Behaviors immediately before occupational fall accidents. *J Occup Saf Health* **16**(1): 11–27 (2023)

[38] Li M S, Melville D, Chung E, Stuart H S. Milliscale features increase friction of soft skin in lubricated contact. *IEEE Robot Autom Let* **5**(3): 4781–4787 (2020)

[39] Hemler S L, Charbonneau D N, Iraqi A, Redfern M S, Haight J M, Moyer B E, Beschorner K E. Changes in under-shoe traction and fluid drainage for progressively worn shoe tread. *Appl Ergon* **80**: 35–42 (2019)

[40] Hemler S L, Charbonneau D N, Beschorner K E. Predicting hydrodynamic conditions under worn shoes using the tapered-wedge solution of Reynolds equation. *Tribol Int* **145**: 106161 (2020)

[41] Gupta S, Chatterjee S, Malviya A, Kundu A, Chanda A. Effect of shoe outsole wear on friction during dry and wet slips: A multiscale experimental and computational study. *Multiscale Sci Eng* **5**(1–2): 62–76 (2023)

[42] Gupta S, Chatterjee S, Chanda A. Effect of footwear material wear on slips and falls. *Mater Today Proc* **62**: 3508–3515 (2022)

[43] Singh G, Beschorner K E. A method for measuring fluid pressures in the shoe–floor–fluid interface: Application to shoe tread evaluation. *IIE Trans Occup* **2**(2): 53–59 (2014)

[44] Matilainen M, Tuononen A. Tyre contact length on dry and wet road surfaces measured by three-axial accelerometer. *Mech Syst Signal Pr* **52–53**: 548–558 (2015)

[45] Beschorner K E, Siegel J L, Hemler S L, Sundaram V H, Chanda A, Iraqi A, Haight J M, Redfern M S. An observational ergonomic tool for assessing the worn condition of slip-resistant shoes. *Appl Ergon* **88**: 103140 (2020)

[46] Cook A, Hemler S, Sundaram V, Chanda A, Beschorner K. Differences in friction performance between new and worn shoes. *IISE Trans Occup Ergon Hum Factors* **8**(4): 209–214 (2020)

[47] Sundaram V H, Hemler S L, Chanda A, Haight J M, Redfern M S, Beschorner K E. Worn region size of shoe outsole impacts human slips: Testing a mechanistic model. *J Biomech* **105**: 109797 (2020)

[48] Walter P J, Tushak C M, Hemler S L, Beschorner K E. Effect of tread design and hardness on interfacial fluid force and friction in artificially worn shoes. *Footwear Sci* **13**(3): 245–254 (2021)

[49] Hemler S L, Pliner E M, Redfern M S, Haight J M, Beschorner K E. Effects of natural shoe wear on traction performance: A longitudinal study. *Footwear Sci* **14**(1): 1–12 (2022)

[50] Hemler S L, Beschorner K E. Validation of a portable shoe tread scanner to predict slip risk. *J Safety Res* **86**: 5–11 (2023)

[51] Li K W, Chen C J. The effect of shoe soling tread groove width on the coefficient of friction with different sole materials, floors, and contaminants. *Appl Ergon* **35**(6): 499–507 (2004)

[52] Gupta S, Chatterjee S, Chanda A. Influence of vertically treaded outsoles on interfacial fluid pressure, mass flow rate, and shoe–floor traction during slips. *Fluids* **8**(3): 82 (2023)

[53] Gupta S, Chatterjee S, Malviya A, Singh G, Chanda A. A novel computational model for traction performance characterization of footwear outsoles with horizontal tread channels. *Computation* **11**(2): 23 (2023)

[54] Li K W, Wu H H, Lin Y C. The effect of shoe sole tread groove depth on the friction coefficient with different tread groove widths, floors and contaminants. *Appl Ergon* **37**(6): 743–748 (2006)

[55] Yamaguchi T, Katsurashima Y, Hokkirigawa K. Effect of rubber block height and orientation on the coefficients of friction against smooth steel surface lubricated with glycerol solution. *Tribol Int* **110**: 96–102 (2017)

[56] Li K W, Chen C J. Effects of tread groove orientation and width of the footwear pads on measured friction coefficients. *Saf Sci* **43**(7): 391–405 (2005)

[57] Blanchette M G, Powers C M. The influence of footwear tread groove parameters on available friction. *Appl Ergon* **50**: 237–241 (2015)

[58] Ishizako A, Tomosada M, Hokkirigawa K, Yamaguchi T. Impact of rubber block end-face corner radius on the friction coefficient between rubber blocks and a glass plate under dry and lubrication conditions. *Tribol Int* **174**: 107705 (2022)

[59] Ishizako A, Matsumoto H, Yamaguchi T. Effect of the end-face corner radius of a rubber block on the friction coefficient and fluid-free gap under glycerin lubrication. *Tribol Int* **184**: 108473 (2023)

[60] Ishizako A, Nishi T, Yamaguchi T. High friction of rubber caused by negative fluid pressure under glycerol lubrication. *Tribol Int* **192**: 109213 (2024)

[61] Yamaguchi T, Umetsu T, Ishizuka Y, Kasuga K, Ito T, Ishizawa S, Hokkirigawa K. Development of new footwear sole surface pattern for prevention of slip-related falls. *Saf Sci* **50**(4): 986–994 (2012)

[62] Yamaguchi T, Hokkirigawa K. Development of a high slip-resistant footwear outsole using a hybrid rubber surface pattern. *Ind Health* **52**(5): 414–423 (2014)

[63] Maegawa S, Itoigawa F, Nakamura T. Effect of surface grooves on kinetic friction of a rubber slider. *Tribol Int* **102**: 326–332 (2016)

[64] Maegawa S, Itoigawa F, Nakamura T. A role of friction-induced torque in sliding friction of rubber materials. *Tribol Int* **93**: 182–189 (2016)

[65] Yamaguchi T, Sugawara T, Takahashi M, Shibata K, Moriyasu K, Nishiwaki T, Hokkirigawa K. Effect of porosity and normal load on dry sliding friction of polymer foam blocks. *Tribol Lett* **66**: 34 (2018)

[66] Moriyasu K, Nishiwaki T, Shibata K, Yamaguchi T, Hokkirigawa K. Friction control of a resin foam/rubber laminated block material. *Tribol Int* **136**: 548–555 (2019)

[67] Roy K, Debnath S C, Potiyaraj P. A critical review on the utilization of various reinforcement modifiers in filled rubber composites. *J Elastom Plast* **52**(2): 167–193 (2020)

[68] Aggarwal A, Hackel N, Grunert F, Ilisch S, Beiner M, Blume A. Investigation of rheological, mechanical, and viscoelastic properties of silica-filled SSBR and BR model compounds. *Polymers* **16**(22): 3212 (2024)

[69] Al-Assi M, Kassem E. Evaluation of adhesion and hysteresis friction of rubber–pavement system. *Appl Sci* **7**(10): 1029 (2017)

[70] Nishi T, Yamaguchi T, Shibata K, Hokkirigawa K. Optimizing the frictional behavior of partially wetting soft contacts as measured with hydrogel covered silicones. *Tribol Int* **153**: 106586 (2021)

[71] Nishi T, Yamaguchi T, Shibata K, Hokkirigawa K. Friction behavior of silicone rubber hemisphere under non-uniform wetting states: With water droplets in air or air bubbles in water. *Tribol Int* **155**: 106769 (2021)

[72] Jones T, Iraqi A, Beschorner K. Performance testing of work shoes labeled as slip resistant. *Appl Ergon* **68**: 304–312 (2018)

[73] Gupta S, Chatterjee S, Malviya A, Chanda A. Traction performance of common formal footwear on slippery surfaces. *Surfaces* **5**(4): 489–503 (2022)

[74] Gupta S, Chanda A. Biomechanical modeling of footwear-fluid-floor interaction during slips. *J Biomech* **156**: 111690 (2023)

[75] Persson B N J. Theory of rubber friction and contact mechanics. *J Chem Phys* **115**(8): 3840–3861 (2001)

[76] Lorenz B, Oh Y R, Nam S K, Jeon S H, Persson B N J. Rubber friction on road surfaces: Experiment and theory for low sliding speeds. *J Chem Phys* **142**(19): 194701 (2015)

[77] Liu X Y, Cao Q Q, Wang H, Chen J Y, Huang X M. Evaluation of vehicle braking performance on wet pavement surface using an integrated tire–vehicle modeling approach. *Transport Res Rec* **2673**(3): 295–307 (2019)

[78] He Y L, Cui Z B, Yang X, Wang C H, Cui K J, Fan Z P, Lu G Y, Lv S T, Wang D W. Investigating intrinsic factors in pavement skid resistance deterioration using an integrated tribology model. *Tribol Int* **199**: 109997 (2024)

[79] Ing H, Chadha V, Randolph A B, Reifler K, Jacobs T D B, Beschorner K E. Validation of a multiscale hysteresis mechanics model in predicting oily shoe-floor friction across surfaces with varying finishes. *J Tribol* **147**(9): 091111 (2025)

[80] Ido T, Yamaguchi T, Shibata K, Matsuki K, Yumii K, Hokkirigawa K. Sliding friction characteristics of styrene butadiene rubbers with varied surface roughness under water lubrication. *Tribol Int* **133**: 230–235 (2019)

[81] Martin P, Silberzan P, Brochard-Wyart F. Sessile droplets at a solid/elastomer interface. *Langmuir* **13**(18): 4910–4914 (1997)

[82] Martin A, Buguin A, Brochard-Wyart F. Dewetting nucleation centers at soft interfaces. *Langmuir* **17**(21): 6553–6559 (2001)

[83] Nishi T, Moriyasu K, Harano K, Nishiwaki T. Influence of dewettability on rubber friction properties with different surface roughness under water/ethanol/glycerol lubricated conditions. *Tribol Online* **11**(5): 601–607 (2016)

[84] Nishi T, Yamaguchi T, Hokkirigawa K. Development of high slip-resistant footwear outsole using rubber surface filled with activated carbon/sodium chloride. *Sci Rep* **12**: 267 (2022)

[85] Nishi T. High friction effect on water-lubricated floor by the addition of silicone rubber particles to diene rubber. *Tribol Int* **176**: 107900 (2022)

[86] Kim D, Yun D. A study on the effect of fingerprints in a wet system. *Sci Rep* **9**: 16554 (2019)

[87] Nishi T, Yamaguchi T, Shibata K, Hokkirigawa K. Friction behavior between an artificial skin block and a glass plate under unlubricated and partly/completely water-lubricated conditions. *Tribol Int* **163**: 107179 (2021)

[88] Hao T Z, Xiao H P, Liu S H, Liu Y B. Fingerprint-inspired surface texture for the enhanced tip pinch performance of a soft robotic hand in lubricated conditions. *Friction* **11**(7): 1349–1358 (2023)

[89] Hao T Z, Xiao H P, Wang J T, Wang X F, Liu S H, Liu Q J. Friction enhancement through fingerprint-like soft surface textures in soft robotic grippers for grasping abilities. *Tribol Lett* **72**(2): 47 (2024)

[90] Drotlef D M, Stepien L, Kappl M, Barnes W J P, Butt H J, del Campo A. Insights into the adhesive mechanisms of tree frogs using artificial mimics. *Adv Funct Mater* **23**(9): 1137–1146 (2013)

[91] Chen H W, Zhang L W, Zhang D Y, Zhang P F, Han Z W. Bioinspired surface for surgical graspers based on the strong wet friction of tree frog toe pads. *ACS Appl Mater Inter* **7**(25): 13987–13995 (2015)

[92] Zhang L W, Chen H W, Guo Y R, Wang Y, Jiang Y G, Zhang D Y, Ma L R, Luo J B, Jiang L. Micro–nano hierarchical structure enhanced strong wet friction surface inspired by tree frogs. *Adv Sci* **7**(20): 2001125 (2020)
[93] Chen D H, Yang X, Zhong M H, Chen C, Wang L H, Wang J C, Weng X H, Li Y W, Chang Z Y. Inspired by tree frog: Bionic design of tread pattern and its wet friction properties. *J Bionic Eng* **19**(4): 1064–1076 (2022)
[94] Guo Y R, Zhang L W, Wang Y, Liang J, Liu X L, Jiang Y G, Jiang L, Chen H W. Nanofiber embedded bioinspired strong wet friction surface. *Sci Adv* **9**(41): eadi4843 (2023)
[95] Mizuhira V. The digital pads of rhacophorid tree-frogs. *J Electron Microsc* **53**(1): 63–78 (2004)
[96] Persson B J. Wet adhesion with application to tree frog adhesive toe pads and tires. *J Phys—Condens Mat* **19**(37): 376110 (2007)
[97] Murarash B, Itovich Y, Varenberg M. Tuning elastomer friction by hexagonal surface patterning. *Soft Matter* **7**(12): 5553–5557 (2011)
[98] Wang Y P, Yang X B, Chen Y F, Wainwright D K, Kenaley C P, Gong Z Y, Liu Z M, Liu H, Guan J, Wang T M, et al. A biorobotic adhesive disc for underwater hitchhiking inspired by the remora suckerfish. *Sci Robot* **2**(10): eaan8072 (2017)
[99] Baik S, Hwang G W, Jang S, Jeong S, Kim K H, Yang T H, Pang C. Bioinspired microsphere-embedded adhesive architectures for an electrothermally actuating transport device of dry/wet pliable surfaces. *ACS Appl Mater Inter* **13**(5): 6930–6940 (2021)
[100] Hwang G W, Lee H J, Kim D W, Yang T H, Pang C. Soft microdenticles on artificial octopus sucker enable extraordinary adaptability and wet adhesion on diverse nonflat surfaces. *Adv Sci* **9**(31): 2202978 (2022)
[101] Ditsche P, Wainwright D K, Summers A P. Attachment to challenging substrates—fouling, roughness and limits of adhesion in the northern clingfish (*Gobiesox maeandricus*). *J Exp Biol* **217**(14): 2548–2554 (2014)
[102] Ishizako A, Nishi T, Yamaguchi T. Effect of orientation and hardness of rubber tread block on the friction coefficient under glycerol lubrication and its underlying mechanisms. *Tribol Int* **198**: 109904 (2024)
[103] Ishizako A, Nishi T, Yamaguchi T. Increasing friction of tread rubber under lubrication by adjusting groove shape to control fluid flow. *Tribol Int* **205**: 110531 (2025)
[104] Groper M, Etsion I. The effect of shear flow and dissolved gas diffusion on the cavitation in a submerged journal bearing. *J Tribol* **123**(3): 494–500 (2001)
[105] Bauer N, Rambaks A, Müller C, Murrenhoff H, Schmitz K. Strategies for implementing the Jakobsson-Floberg-Olsson cavitation model in EHL simulations of translational seals. *Int J Fluid Power* **22**(2): 199–232 (2021)

Arata Ishizako received his Ph.D. degree in mechanical engineering from Tohoku University, Japan, in 2025. He is currently an assistant professor at the Graduate School of Engineering, Tohoku University. His research interests include friction control of soft materials under lubrication.

Toshiaki Nishi has been an associate professor at Tohoku University, Japan, since 2025. He is mainly engaged in research and development related to the friction and wear characteristics of soft matter, including rubber, polymers, hydrogels, and biological materials. His research interests include the design of materials and structures on the basis of the distributions of wetting and strain. He received his master degree in chemistry from Kyoto University, Japan, in 2011 and worked at ASICS Corporation, Japan, from 2011 to 2023. In 2021, he completed his doctoral degree in fine mechanics at the Graduate School of Engineering, Tohoku University. He worked at Tohoku University as an assistant professor from 2023 to 2024.

Takeshi Yamaguchi is currently a full professor of mechanical engineering and biomedical engineering at Tohoku University, Japan. He received his B.S., M.S., and Ph.D. degrees in engineering at Tohoku University in 1999, 2000, and 2008, respectively. He was an assistant professor from 2000 to 2010 and an associate professor at Tohoku University from 2011 to 2021. He studied at the University of Toronto, Canada, as a visiting researcher from 2010 to 2011. He has been interested in the tribology of soft materials, including footwear friction and biomechanics, in human locomotion.